

## Nuclear Spin Ordering on the Surface of a $^3\text{He}$ Crystal: Magnetic Steps

I. A. Todoshchenko, H. Alles,\* H. J. Junes, M. S. Manninen, and A. Ya. Parshin<sup>†</sup>

*Low Temperature Laboratory, Helsinki University of Technology, P. O. Box 5100, 02015 TKK, Finland*

(Received 21 April 2009; published 18 June 2009)

The growth rates of the (110) and (100) facets on bcc  $^3\text{He}$  crystals have been measured near the magnetic ordering transition at  $T_N = 0.93$  mK. In the ordered phase, we have observed several growth modes which correspond to different values of the step energy. We show that, because of quantum delocalization, the step induces a cluster of ferromagnetically ordered nuclear spins. The free energy of such a cluster is relatively large and depends on the orientation of the underlying antiferromagnetic domain. In the paramagnetic phase, the mobilities of the basic facets are greatly reduced because of the much slower spin diffusion in the bulk solid.

DOI: 10.1103/PhysRevLett.102.245302

PACS numbers: 67.80.-s, 75.70.Rf, 81.10.Aj

Helium represents an excellent model system to study crystal surfaces because the solid-liquid interface of helium can be cooled down to very low temperatures at which the liquid is superfluid and the mass and heat transport are efficient. Thus, in contrast to usual crystals, the intrinsic properties of the surface of helium crystals are not masked by the dissipation in the bulk phases and can be directly studied. In addition, at low temperatures helium samples are extremely pure.

Faceting is probably the most interesting phenomenon taking place on the crystal surface. Facets are smooth planes in the high symmetry directions of the crystal lattice. They reflect the discrete nature of the crystal and appear on the crystal surface due to the strong anisotropy of growth. The rough crystal surface grows easily because of the large number of sticking sites for atoms. In contrast, smooth facets grow slowly, through the motion of elementary steps which separate terraces of different atomic layers. Steps are typically present on facets due to screw dislocations. The growth rate of a facet depends on the parameters of an elementary step, such as its height  $d$  and free energy per unit length  $\beta$ .

The growth dynamics of  $^4\text{He}$  crystals at low temperatures has been intensively studied in the series of works by Ruutu *et al.* (for a review and references, see [1]). However, for such investigations  $^3\text{He}$  crystals present an even more interesting system because of nuclear spins which order antiferromagnetically at the Néel temperature  $T_N = 0.93$  mK. Thus  $^3\text{He}$  provides a unique opportunity to investigate the influence of the magnetic structure of a crystal on the properties of its surface.

In our earlier work, we have measured the growth rates of different types of facets on bcc  $^3\text{He}$  crystals at 0.55 mK. The velocities of the facets were found to depend linearly on the applied overpressure, and the mobilities of facets showed strong anisotropy [2]. These data were interpreted in terms of spiral growth in the regime of saturated step velocity, and the step energies for ten different types of facets were extracted.

In this Letter, we describe a series of measurements on the growth dynamics of the basic (110) and (100) facets on bcc  $^3\text{He}$  crystals in the vicinity of  $T_N$  in the temperature range of 0.55–1.2 mK. In the ordered phase, we have observed that both facet types may possess several different growth modes. We suggest that the step induces a ferromagnetic polaron whose properties depend on the orientation of the underlying antiferromagnetic domain. In the paramagnetic phase, the mobilities of both types of facets decrease because the spin transport associated with the motion of a polaron is much slower than in the ordered phase.

In our measurements we used the interferometric setup described in detail in Ref. [3]. The  $^3\text{He}$  crystals were nucleated at a constant temperature by pressurizing the liquid over the melting pressure value in the presence of a high voltage applied to a sharp tungsten tip. The nucleated crystal seeds were first grown to a size of about 3 mm and then melted in order to have a rounded surface, after which they were grown at different compression rates. Since rough surfaces grow fast, crystals quickly became faceted. After that, relatively fast high order facets started to disappear from the crystal surface, until only the two slowest, basic types of facets, (110) and (100), remained.

Our first qualitative experiment was a cooling of the growing  $^3\text{He}$  crystal through  $T_N$  with a constant compression rate. The changes in the positions of facets were determined by following the interference fringes corresponding to each facet. Altogether six facets were followed during this experiment, three of (110) and three of (100) type. The normal displacements of all six facets versus time and the corresponding pressure trace are shown in Fig. 1. During cooling, pressure in the liquid varies due to the slope of the melting curve which becomes much smaller below  $T_N$  because of the entropy drop in the solid phase. Thus the abrupt decrease of a slope of the pressure trace at  $t \approx 1600$  s indicates the spin-ordering transition (dashed vertical line in Fig. 1).

As seen from Fig. 1, the nuclear ordering transition makes a pronounced effect on the growth dynamics of

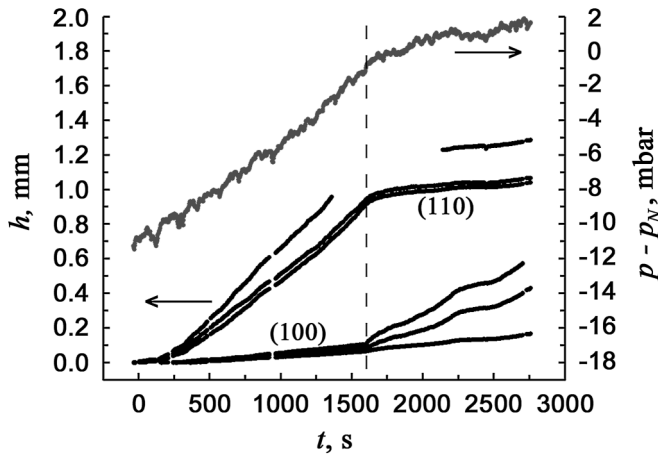


FIG. 1. Normal displacements  $h$  of 6 different facets during fast cooling of a growing  $^3\text{He}$  crystal through  $T_N$ . The gray line indicates the variation of pressure  $p$  in the cell with respect to the melting pressure at the ordering transition  $p_N$ . The dashed vertical line marks the nuclear ordering transition.

$^3\text{He}$  crystals. Above  $T_N$ , facets of the (100) type grow much more slowly than the ones of the (110) type, whereas in the ordered phase the situation is inverted: The slowest facets are of the (110) type. It is also clear that the velocities of different (100) facets are different in the ordered phase.

In contrast to the first experiment, the crystal shown in Fig. 2 was nucleated and grown first below  $T_N$ , at 0.86 mK, where its growth shape showed the slowest horizontal (110) facet on top. After warming the crystal slowly above  $T_N$  to 1.06 mK, the faceting of the growth shape appeared to be completely different: The crystal became covered with only (100) facets. All other facets grew much faster, and the crystal took the shape of a perfect cube. Cooling down below  $T_N$  to 0.90 mK recovered the faceted shape back, with the large (110) facet on top of the crystal. Final

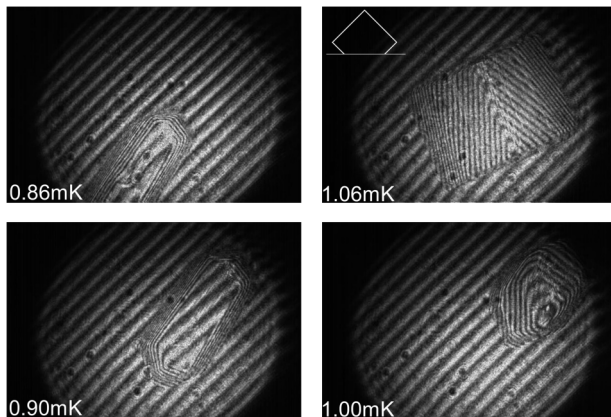


FIG. 2. Interferograms of a growing  $^3\text{He}$  crystal at different temperatures below and above the ordering transition at  $T_N = 0.93$  mK. The sequence of temperatures was 0.86, 1.06, 0.90, and 1.00 mK.

warming up through  $T_N$  to 1.00 mK made the crystal again covered mostly with the (100) facets.

The growth resistance of the solid-liquid interface generally consists of two parts: (i) the intrinsic isothermal resistance of the interface and (ii) the so-called “bulk resistance,” which is due to the release of latent heat, finite thermal conductivity of the bulk phases, and the Kapitza resistance between the two phases [4,5]. In an experiment, one typically measures the total growth resistance. However, in the millikelvin temperature range the bulk resistance, which corresponds to the growth (or melting) of the rough surface, is much smaller than the growth resistances of the basic types of facets [3,6,7]. Thus the chemical potential difference  $\Delta\mu$  across the interface which drives the growth is simply proportional to the excess pressure  $\delta p$  over the equilibrium melting pressure:  $\Delta\mu = \delta p(1/\rho_l - 1/\rho_s)$ , where  $\delta p = p - p_{MC}(T)$  and  $\rho_l$  and  $\rho_s$  are the mass densities of the liquid and solid, respectively [8].

Measurements on the mobility of the solid-liquid interface of  $^3\text{He}$  at temperatures near the ordering transition are rather difficult because the latent heat of crystallization is remarkable and the temperature in the experimental cell varies in the course of growth. Thus, the measurements on the driving overpressure  $\delta p$  during crystal growth require careful tracking of the temperature changes in the cell. To follow the temperature, we have used a vibrating wire thermometer which was calibrated against the equilibrium melting pressure (for details, see [9]). This allowed us to extend our measurements of the growth dynamics of  $^3\text{He}$  crystals from our lowest available temperature of 0.55 mK up to about 1.2 mK.

We have performed measurements with 7 different crystals and with more than 20 different facets of the (110) and (100) types. In order to detect a possible history-dependent behavior, we examined different sequences of measurements. Some of the experiments were carried out with one and the same crystal at different temperatures both below and above  $T_N$ . Other experiments were done with crystals which were nucleated at temperatures very close to the temperature of the growth experiment. The velocity-overpressure dependencies measured in the magnetically ordered phase are shown in Fig. 3.

We have observed that at  $T < T_N$  both (110) and (100) facets may grow in different modes. We were not able to detect a certain dependence of the growth mode on the temperature or history of the sample. On one and the same crystal, two different facets of the same type may grow at the same time with different velocities. In addition, after several growth and melting sequences, facets may switch from one growth mode to another.

The velocities of the facets depend linearly on the applied overpressure and, following Tsepelin *et al.* [2], we interpret our data with spiral growth due to the motion of steps created by screw dislocations:

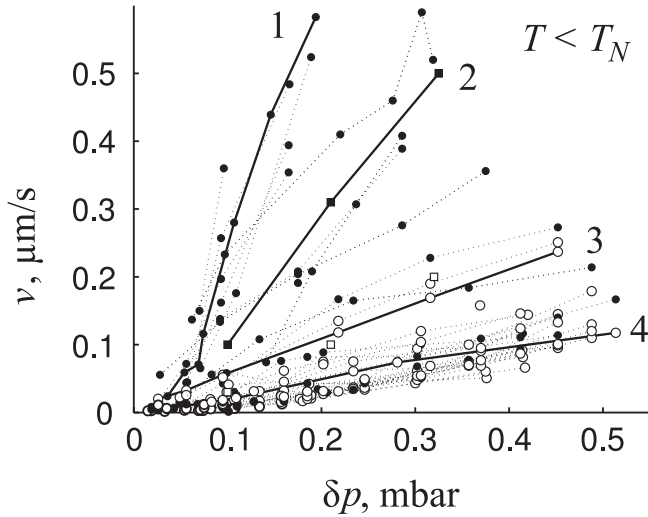


FIG. 3. Normal velocities of the (110) (open symbols) and (100) (filled symbols) facets in the magnetically ordered phase  $0.55 \text{ mK} < T < 0.93 \text{ mK}$  measured in this work (circles) and by Tsepelin *et al.* [2] at  $0.55 \text{ mK}$  (squares). Two fast growth modes (characteristic traces are shown with solid lines 1 and 2) are seen for the (100) facet and one fast mode (trace 3) for the (110) facet. The slow modes are similar for both types of facet (trace 4). Several traces correspond to transitional modes.

$$v = \frac{v_c d^2}{2\pi\beta} \frac{\rho_s - \rho_l}{\rho_l} \delta p. \quad (1)$$

Here  $v_c$  is the critical velocity of the step, which in the ordered phase is the magnon velocity  $v_c \approx 7 \text{ cm/s}$  [3].

We note that in the spin-ordered phase the facets of the same type may physically differ, because they may have different orientations with respect to the direction of the spin ordering. Despite the fact that the nuclear spin exchange energy in the solid  $I_s \approx 1 \text{ mK}$  is much smaller than the step energies of the basic facets  $\beta_{110} = 6.6 \times 10^{-10} \text{ erg/cm}$  and  $\beta_{100} = 1.4 \times 10^{-10} \text{ erg/cm}$  [2], quantum delocalization effects could change the step energies significantly. As is well known, a vacancy in the bulk solid  ${}^3\text{He}$  forms in its vicinity a macroscopic ferromagnetically ordered cluster [10], the so-called polaron. Such a vacancy greatly enhances the exchange between neighboring atoms  $J \gg I_s$ . The size  $R$  of the ferromagnetic cluster is set by the competition between the localization energy  $\sim J(a/R)^2$  and the excess in the magnetic energy  $\sim I_s(R/a)^3$ . On atomically rough crystal surfaces, vacancies are present with high concentrations which leads to the ferromagnetic ordering of the boundary layer [11,12].

The elementary step can also be viewed as a rough surface with width  $\xi$  [13], where the concentrations of vacancies and adatoms in the boundary layer of the crystal are of the order of unity (see Fig. 4). The step thus induces a ferromagnetically ordered band of spins in its vicinity with the energy of localization  $\sim Ja/\xi^2$  (per unit length of the step). Another contribution to the energy of the cluster

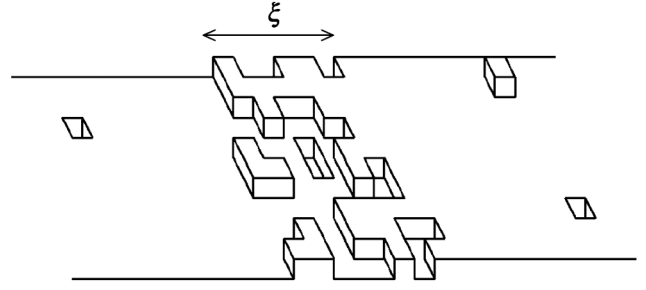


FIG. 4. Elementary step viewed as a rough surface with the width  $\xi$  of several interatomic distances. Delocalization of the surface vacancies leads to the ferromagnetic ordering of spins in the vicinity of the step, similarly to the formation of the ferromagnetic polaron near the vacancy in the bulk solid.

is the loss in the magnetic energy because of the destruction of the antiferromagnetic ordering:  $I_s \xi l/a^3$  ( $l \lesssim \xi$  is the depth of the cluster). If the exchange effects dominate, they set the width of the step  $\xi \approx a(2J/I_s)^{1/4}$  and its energy  $\beta^* \approx \sqrt{8JI_s}/a$ . Mobile surface vacancies provide a relatively strong exchange  $J \sim 1 \text{ K}$  on the rough surface [11], which yields the value of the step width  $\xi \sim 7a$  and the value of the magnetic energy of the step  $\beta^* \sim 4 \times 10^{-10} \text{ erg/cm}$ . The estimated magnetic energy is thus comparable to the step energy of the basic (110) facet which means that the surface exchange effects are significant even for low order facets.

The picture described above can explain the observed multitude of growth modes of the basic facets in the ordered phase. The magnetic structure of bcc solid  ${}^3\text{He}$  below  $T_N$  consists of ferromagnetically ordered (100) planes in the sequence up-up-down-down (u2d2). Thus, there can be two physically different (100) facets: (i) a ferromagnetic one which coincides with one of the ferromagnetic planes and (ii) an antiferromagnetic one which is perpendicular to the ferromagnetic planes. Facets of the (110) type can also be of two kinds, both antiferromagnetic: (i) a facet tilted by  $45^\circ$  with respect to the ferromagnetic planes and (ii) a facet perpendicular to the ferromagnetic planes.

The calculations of the particular values of the step energies for these four different kinds of (110) and (100) facets are very much involved. However, some relations between them could be obtained with qualitative arguments. In the case of a ferromagnetically ordered (100) facet, the step may separate terraces either with identical or with opposite orientations of the magnetization. In the first case the localization effects are absent, and the magnetic energy of the step is small (the fastest growth mode 1 in Fig. 3). In the second case the step has an additional magnetic energy due to the local destruction of the ferromagnetic order (the second fastest mode 2). For the steps on the antiferromagnetically ordered facets, the localization effects are strong, and they have large magnetic energy, of the order of  $\beta^* \approx \sqrt{8JI_s}/a$ . It is also reasonable to

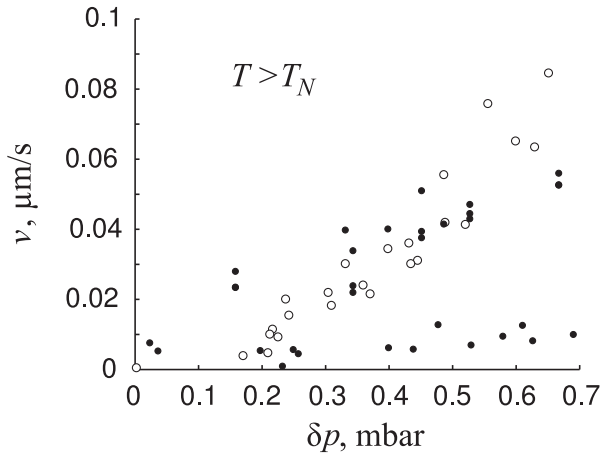


FIG. 5. Normal velocity of the (110) (open symbols) and (100) (filled symbols) facets in the paramagnetic phase  $0.93 \text{ mK} < T < 1.2 \text{ mK}$ .

suggest that facets of the (100) and (110) types which are perpendicular to the ferromagnetic planes of the u2d2 structure have similar step energies (the growth mode 4 in Fig. 3).

The described model of a magnetic step suggests that in the paramagnetic phase all facets of the same type are equivalent and that the step energies of both the (110) and (100) facets are nearly equal and somewhat smaller than in the ordered phase. Our results obtained in the paramagnetic phase are shown in Fig. 5. Indeed, most of the growth data for both facets are very similar. The slope which is proportional to  $v_c/\beta$  is about 2 times smaller than the slope of the slowest mode below  $T_N$ . In the disordered phase the maximum velocity of the step is set by the spin diffusion. The motion of the ferromagnetic step with the velocity  $v_{st}$  induces the spin current in the solid near the step, with characteristic density  $j \sim v_{st}/a^3$ . Since the driving spin density gradient is of the order of  $1/(\xi a^3)$ , the maximum velocity of the step in the paramagnetic phase is  $v_{max} \approx D/\xi \approx 0.5 \text{ cm/s}$  ( $D \approx 10^{-7} \text{ cm}^2/\text{s}$  is the spin diffusion coefficient in the paramagnetic phase [14]), which is by an order of magnitude smaller than the critical velocity in the ordered state. In Eq. (1) for the facet velocity, the decrease of the maximum velocity is partly compensated by the decrease in the step energy. As a result, the velocities of the (110) and (100) facets are only twice smaller in the paramagnetic phase than in the ordered phase.

Some of the (100) facets are, however, much slower above  $T_N$ , with the slope by an order of magnitude smaller than the slope of the slowest mode in the ordered phase. We guess that these facets are spontaneously u2d2 ordered even at temperatures slightly above  $T_N$ , since the exchange energy near the surface is somewhat larger than in the bulk. For the (100) facet perpendicular to the ferromagnetic planes, the value of the step energy remains roughly the same as in the ordered phase, but the maximum velocity of

the step is by an order of magnitude smaller than in the antiferromagnetic state.

In summary, we have measured the mobilities of the basic (110) and (100) facets on  $^3\text{He}$  crystals in a wide temperature range near the magnetic ordering transition. We have observed several growth modes in the ordered phase which we explain by the formation of ferromagnetic clusters in the solid near the steps. The step may thus have different energies depending on the orientation of the magnetic domain. In the disordered phase the mobilities are reduced because in the absence of bulk magnons the maximum velocity of the steps is set by the spin diffusion and is much smaller than in the ordered phase. We would like to point out that the effect of the nuclear spins on the step energy is greatly enhanced due to quantum delocalization, and such an influence has never been observed before.

This work was supported by the EC-funded ULTI project, Transnational Access in Program FP6 (Contract No. RITA-CT-2003-505313), and by the Academy of Finland (Finnish Centre of Excellence Program 2006–2011 and the Visitors Programs No. 111895 and No. 117710).

\*Present address: Institute of Physics, University of Tartu, Riia 142, 51014 Tartu, Estonia.

†Present address: P.L. Kapitza Institute, Kosygina 2, Moscow 119334, Moscow Institute for Physics and Technology, Institutskii 9, Dolgoprudnyi 141700, Russia.

- [1] J. P. Ruutu, P. J. Hakonen, A. Babkin, A. Y. Parshin, and G. Tvalashvili, *J. Low Temp. Phys.* **112**, 117 (1998).
- [2] V. Tsepelin, H. Alles, A. Babkin, R. Jochemsen, A. Y. Parshin, and I. A. Todoshchenko, *Phys. Rev. Lett.* **88**, 045302 (2002).
- [3] V. Tsepelin, H. Alles, A. Babkin, R. Jochemsen, A. Y. Parshin, and I. A. Todoshchenko, *J. Low Temp. Phys.* **129**, 489 (2002).
- [4] F. Graner, S. Balibar, and E. Rolley, *J. Low Temp. Phys.* **75**, 69 (1989).
- [5] P. Nozières and M. Uwaha, *J. Phys. (Paris)* **48**, 389 (1987).
- [6] R. Nomura, H. H. Hensley, T. Matsushita, and T. Mizusaki, *J. Low Temp. Phys.* **94**, 377 (1994).
- [7] H. Akimoto, R. Rooijen, A. Marchenkov, R. Jochemsen, and G. Frosatti, *Physica (Amsterdam)* **255B**, 19 (1998).
- [8] V. I. Marchenko and A. Y. Parshin, *JETP* **52**, 129 (1980).
- [9] I. A. Todoshchenko, H. Alles, A. Babkin, A. Y. Parshin, and V. Tsepelin, *J. Low Temp. Phys.* **126**, 1449 (2002).
- [10] A. F. Andreev, *JETP Lett.* **24**, 564 (1976).
- [11] A. E. Meyerovich and B. Z. Spivak, *JETP Lett.* **34**, 551 (1981).
- [12] S. V. Iordanskii and A. V. Smirnov, *JETP Lett.* **32**, 398 (1980).
- [13] P. Nozières and F. Gallet, *J. Phys. (Paris)* **48**, 353 (1987).
- [14] B. Cowan and M. Fardis, *Physica (Amsterdam)* **165B–166B**, 823 (1990).